Chemical Science

ROYAL SOCIETY OF CHEMISTRY

EDGE ARTICLE

View Article Online
View Journal | View Issue

Cite this: *Chem. Sci.*, 2023, **14**, 11381

All publication charges for this article have been paid for by the Royal Society of Chemistry

Received 10th July 2023
Accepted 18th September 2023

DOI: 10.1039/d3sc03528j

rsc.li/chemical-science

Directing group assisted *para*-selective C–H alkynylation of unbiased arenes enabled by rhodium catalysis†

Uttam Dutta,‡[a] Gaurav Prakash,‡[a] Kirti Devi,[a] Kongkona Borah,[a] Xinglong Zhang *[b] and Debabrata Maiti *[a]

Regioselective C–H alkynylation of arenes *via* C–H activation is challenging yet a highly desirable transformation. In this regard, directing group assisted C(sp^2)–H alkynylation of arenes offers a unique opportunity to ensure precise regioselectivity. While the existing methods are mainly centered around *ortho*-C–H alkynylation and a few for *meta*-C–H alkynylation, the DG-assisted *para*-selective C–H alkynylation is yet to be reported. Herein we disclose the first report on Rh-catalyzed *para*-C–H alkynylation of sterically and electronically unbiased arenes. The *para*-selectivity is achieved with the assistance of a cyano-based directing template and the selectivity remained unaltered irrespective of the steric and electronic influence of the substituents. The post-synthetic modification of synthesized *para*-alkynylated arenes is also demonstrated. The mechanistic intricacies of the developed protocol are elucidated through experimental and computational studies.

The acetylene motif is prevalent in various natural products, agrochemicals, pharmaceuticals, and in materials.[1] It not only provides a unique linear and rigid backbone in molecular arrangement but it also renders a platform to harness the benefit of the extended π-conjugated system in organo-electronic materials.[2] The easily transformable nature of the alkyne is an additional advantage as it offers a unique opportunity to diversify the drug molecules and biologically active molecules *via* triple bond functionalization.[3] Therefore, alkynylation of arenes is considered as one of the most desirable transformations. In this regard, the palladium catalyzed Sonogashira coupling reaction is the most versatile and generalized method to synthesize aryl alkynes using aryl (pseudo)halides and terminal alkynes.[4] However, utilization of prefunctionalized aryl(pseudo)halides is the major drawback of this method and it inhibits wide application in synthetic chemistry.

In search of alternative approaches that preclude the usage of prefunctionalized arenes, a number of methods were developed in which arene-C(sp^2)–H alkynylation was achieved using terminal alkynes or activated alkynes, *e.g.* ethynylbenziodoxolone (EBX) reagents[5] or haloalkynes.[6] Notably, the success of these methods requires electronically activated arenes[7] or arenes bearing a chelating directing group (DG).[8] While the former strategy delivers an alkynylated product based on the electronic effect of its substituents, the latter ensures the regioselective alkynylation of the targeted arene depending on the nature of the directing group. The applicability of the electronically controlled C(sp^2)–H alkynylation method is limited to a certain class of substrates bearing electron releasing functional groups. Contrary to that, the DG-assisted C–H activation strategy offers a broad scope and practical method to ensure regioselective C–H alkynylation. However, the majority of the available methods are limited to *ortho*-C–H alkynylation, which proceed *via* a thermodynamically favourable five to six membered metallacyclic intermediate. Examples pertaining to the DG-assisted distal *meta*- or *para*-C–H alkynylation, which proceeded *via* a large macrocyclic cyclophane-type intermediate,[9] are scarce in the literature. However, the state-of-the art methodologies that are available to perform *para*-selective C–H functionalization of arenes, either rely on the electronic control of the arene or the prudent design of the templates. In this regard, *para*-selective borylation was achieved by the group of Itami with the help of an elegantly designed bulky ligand.[10] The group of Nakao reported the *para*-selective alkylation and borylation under nickel[11] and iridium[12] catalyzed conditions, respectively, by exploiting the steric governance of Al-based Lewis acids. A specialized L-shaped template was developed by Chattopadhyay and co-workers to perform *para*-selective borylation of aromatic esters.[13] *Para*-selective alkylation of aniline derivatives was demonstrated by Frost under Ru-catalyzed conditions in 2017.[14] Subsequently, a similar

[a]*IIT Bombay, Department of Chemistry, Powai, Mumbai 400076, India. E-mail: dmaiti@iitb.ac.in*

[b]*Institute of High Performance Computing (IHPC), Agency for Science, Technology and Research (A*STAR), Singapore, Singapore. E-mail: zhang_xinglong@ihpc.a-star.edu.sg*

† Electronic supplementary information (ESI) available. See DOI: https://doi.org/10.1039/d3sc03528j

‡ These authors contributed equally.

catalytic platform was used by Zhao to perform *para*-selective difluoromethylation of anilides[15] and ketoximes.[16] In 2020, they also reported *para*-selective difluoromethylation using iron(-tetraporphyriinato) chloride [Fe(TPP)Cl].[17] Evidently, these protocols are extremely limited to a certain class of substrates as well as functionalizations. In order to establish a robust protocol to access selective distal C–H alkynylation of sterically and electronically unbiased arenes, we rely on the directing group assisted C–H activation technique. The group of Yu, in this regard, has demonstrated a *meta*-C–H alkynylation protocol using an *ortho*-directing group under palladium-norbornene (Pd-NBE) cooperative catalysis.[18] Our group has also developed *meta*-selective alkynylation protocols employing previously developed *meta*-directing groups under both palladium[19a] and rhodium[19b] catalyzed conditions. However, the notable development in the realm of selective *para*-C–H alkynylation is yet to be reported.

A suitable directing group to ensure the selective *para*-C–H activation requires to maintain a precise geometric orientation between the desired C–H bond and the directing group, so that the transition metal catalyst can be accommodated at the proximity of the desired *para*-C–H bond.[9c,20] In this regard, a cyano-based D-shaped template was contemplated by our group in 2015 to execute the *para*-selective C–H functionalization.[20] With this D-shaped template, thus far, *para*-selective C–H olefination,[20,21a] acetoxylation,[20,21b] silylation,[21c] ketonization,[21d] cyanation,[21e] and arylation[21f] have been achieved. In 2021, Li and coworkers developed a novel pyridine-based *para*-directing template to harness *para* selective olefination under Pd-catalyzed conditions.[22] Despite the seminal progress in this realm, the widespread application of the template assisted *para*-selective C–H activation is yet to be achieved. We, therefore, became interested in harnessing *para*-selective C–H alkynylation of arenes by employing the D-shaped template. Nevertheless, *para*-selective alkynylation of aniline derivatives was achieved by Waser[7c] and Fernández-Ibáñez[7d] using Au and Pd catalysts, respectively. These methods were found to be effective with electron rich aniline derivatives. van Gemmeren and coworkers also reported sterically controlled C–H alkynylation of arenes under Pd-catalyzed conditions at the distal *meta*-position.[23]

Our investigation in *para*-selective C–H functionalization relying on template assistance is mainly centered around the palladium catalyzed conditions in combination with the super stoichiometric silver oxidant.[20,21] In sharp contrast, broader catalytic potential of other transition metals is yet to be explored. To the best of our knowledge, *para*-selective C–H olefination is the only instance, reported to date under Rh-catalyzed conditions (Scheme 1a).[24] As our concerted focus is devoted to diversifying the template assisted regioselective distal C–H functionalization method, herein we disclosed the first example of DG-assisted *para*-C–H alkynylation of arenes *via* an inverse Sonogashira coupling reaction utilizing a Rh-catalyst (Scheme 1b). More importantly, the desired transformation is unattainable under Pd-catalyzed conditions. Therefore, the present method provides a complementary platform to Pd-catalysis in achieving selective distal C–H functionalization of arenes.

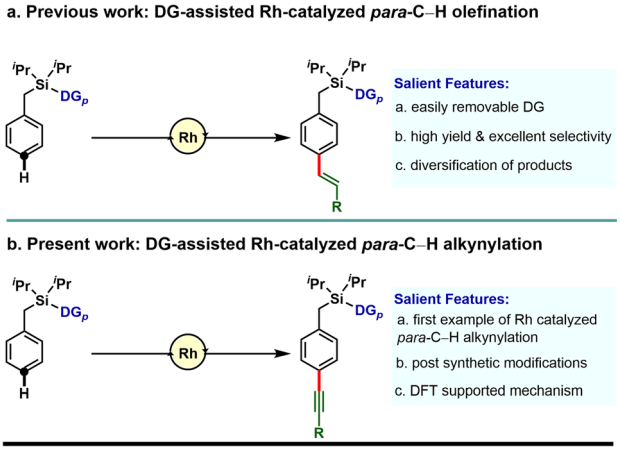

Scheme 1 Directing group assisted Rh catalyzed *para*-C–H functionalization of arenes.

To demonstrate the feasibility of the *para*-selective C–H alkynylation reaction, we chose a model toluene scaffold, equipped with the electron rich, dimethoxy substituted cyano-based D-shaped template ($\mathbf{DG_1}$) and (bromoethynyl)triisopropylsilane as an alkynylating coupling partner. Initial attempt of *para*-C–H alkynylation using $[RhCp^*Cl_2]_2$ as catalyst, $CuCl_2$ as oxidant and Ag_2CO_3 as co-oxidant in the presence of trifluoroacetic acid (TFA) in dichloroethane (DCE) solvent gave the desired product in 20% yield. While optimizing the Rh-catalysts, a slight improvement in yield was observed with $[Rh(COD)Cl]_2$. $Rh_2(OAc)_4$ and $Rh(PPh_3)_3Cl$ were found to be ineffective. Further optimization of the reaction parameters revealed that the combination of dual additives consisting of $Cu_2Cr_2O_5$ and Ag_2SO_4 furnished the desired compound in 51% yield. Finally, synthetically useful yield (76% isolated) and selectivity (*para* : others >15 : 1) were achieved when a combination of 1-adamantanecarboxylic acid and Na_2CO_3 was used as an acid and base additive, respectively. We also tried using oxygen as a green oxidant along with a catalytic amount of $Cu_2Cr_2O_5$ but the reaction outcome was not good compared to $Cu_2Cr_2O_5$ as the stoichiometric oxidant.[25] Notably, electronically modified cyano-based weakly coordinating directing groups (**DG2**, **DG3**, and **DG4**) were also examined and all of them were found to be less efficient in comparison to **DG1** (Table 1). Additionally, relatively strongly coordinating pyridine (**DG5**), pyrimidine (**DG6**) and quinoline (**DG7**) based directing groups failed to produce the alkynylated compounds under the developed reaction conditions.

With the optimized reaction conditions, the mono substituted toluene-based scaffolds tethered with **DG1** were examined to demonstrate the generality of the developed method (Scheme 2). Both the electron donating as well as electron withdrawing substituents delivered the desired *para*-alkynylated compounds with excellent yield and acceptable selectivity.

The electron releasing methyl substituent provided the desired product (**2b**) in 79% yield with greater than 15 : 1 selectivity and the electron deficient haloarenes (**2c–2e**) and *ortho*-trifluoromethyl arene also gave the *para*-alkynylated

Table 1 Directing group (DG) optimization

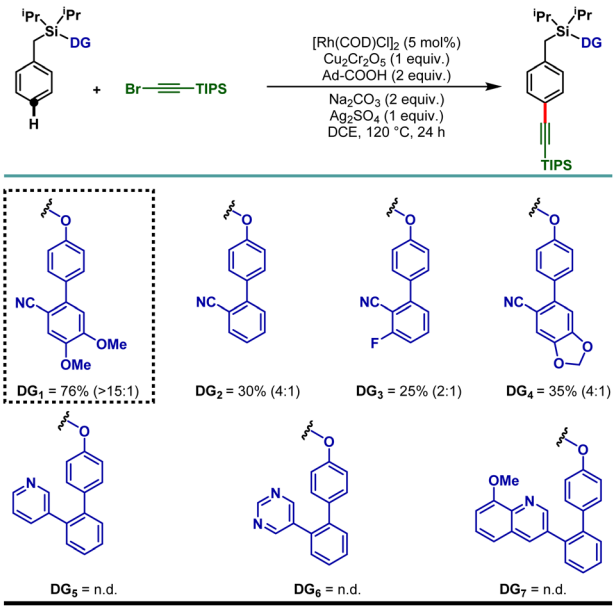

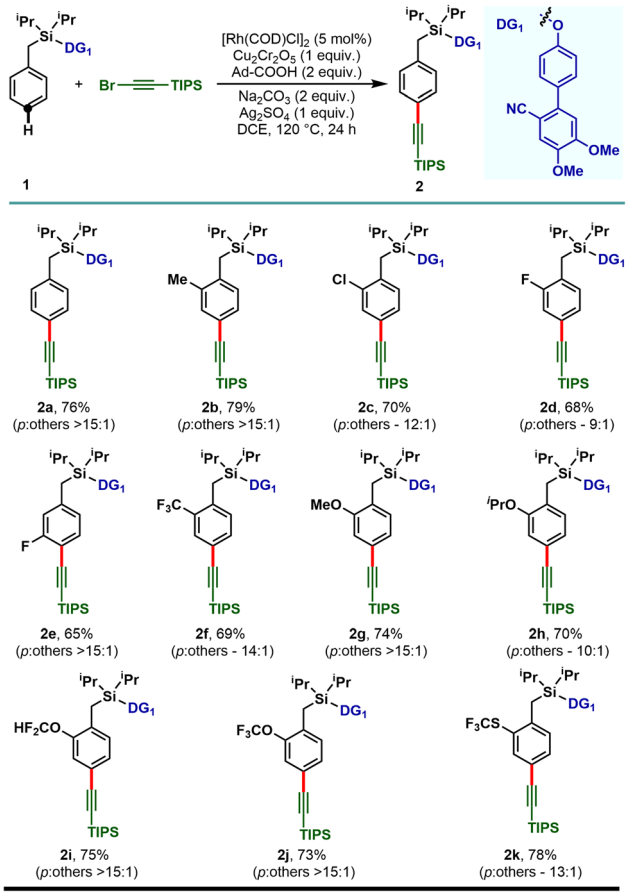

Scheme 2 Rh-catalyzed *para*-C–H alkynylation of mono-substituted arenes.

compounds (**2f**) in good yield and selectivity. Additionally, arenes bearing ethers (**1g–1j**) and thioether (**1k**) were tolerated under the reaction conditions and the desired products were obtained without compromising the yield and selectivity. The versatility of the developed protocol was further demonstrated with disubstituted arenes. *para*-C–H alkynylation with both the 2,6- (**1l–1p**) and 2,5-disubstituted arenes (**1q–1s**) proceeded smoothly and the desired products were obtained in synthetically useful yield and selectivity (Scheme 3). Notably, while the *meta*-F substrate provided the *para*-alkynylated compound in 65% yield with >15 : 1 selectivity, relatively bulky *meta*-substituents such as *meta*-CH_3, *meta*-Cl, and *meta*-CF_3 scaffolds delivered mainly the *meta*-alkynylated compounds. We reasoned that the bulkiness of these substituents prevents the accessibility of the *para*-C–H bond and therefore the sterically less hindered *meta*-C–H bond was activated. Further, the applicability of the protocol was extended to α-substituted toluene derivatives (**1t** and **1u**). Notably, the α-phenyl toluene derivative mainly afforded the mono-alkynylated product (**2t**, mono : di – 10 : 1). It is evident from the scope of the reaction that the electronic nature of the arenes and steric influence of the substituents did not alter the reaction outcome in terms of yield and *para*-selectivity. Thus, the protocol offers an opportunity to expand the scope of regioselective distal *para*-C–H alkynylation to accommodate a wide range of steric and electronic demands of substrates. However, the developed protocol failed to accommodate other alkyne coupling partners such as 1-bromo-2-phenylacetylene, 1-bromohept-1-yne, ethyl 3-bromopropiolate and (bromoethynyl) trimethylsilane. The phenomenon could be justified by the

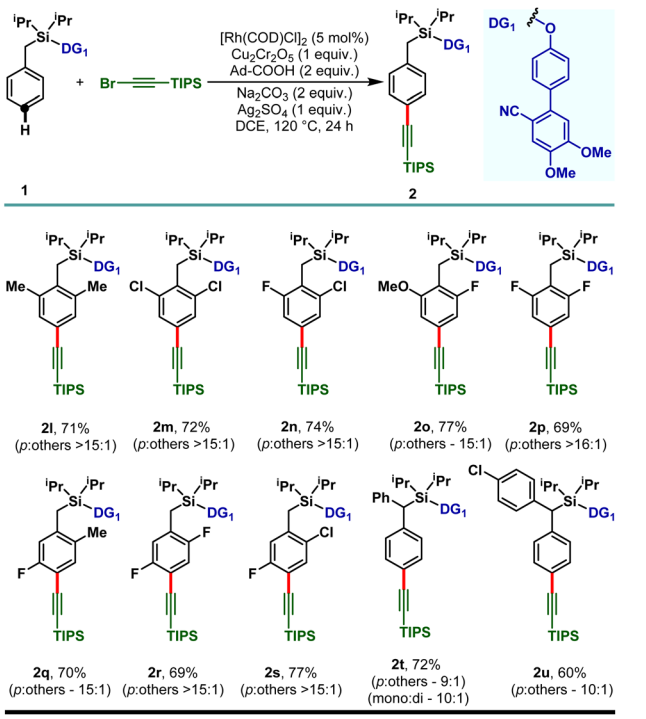

Scheme 3 Rh-catalyzed *para*-C–H alkynylation of di-substituted arenes.

coordinating propensity of π bonds to the Rh center, which was also highlighted in the previous literature reports.[26]

The synthetic utility of the developed *para*-selective C–H alkynylation protocol was further demonstrated through the removal of the appended directing group as well as through functional group interconversion (Scheme 4). Treatment of **2a** with tetra-butylammonium fluoride (TBAF) furnished *p*-tolylacetylene (**3**) along with the directing group (**DG1**) in quantitative yield. It is worth noting that the 4′-hydroxy-4,5-dimethoxy-[1,1′-biphenyl]-2-carbonitrile (DG_1) could be attached further to prepare our starting materials, highlighting the reusability of the directing group. Compound **2a** treated with *p*-toluenesulfonic acid in methanol resulted in a silanol derivative, **4**. Taking advantage of *ortho*-directing capability of the silanol motif, **4** was subjected to Pd catalyzed *ortho*-C–H olefination reaction conditions and an *ortho*-olefinated and *para*-alkynylated compound, **5** was obtained in 68% yield. Considering the easy transformability of alkynes, the alkynylated product (**3**) was reduced to corresponding alkane (**6**) and alkene (**7**), and oxidized to benzonitrile (**8**), benzoic acid (**9**), and phenyl acetic acid (**10**) derivatives. Additionally, oxynitration (**11**), oxydibromination (**12**), and cyclopropenation (**13**) reactions were also achieved with good to excellent yields.

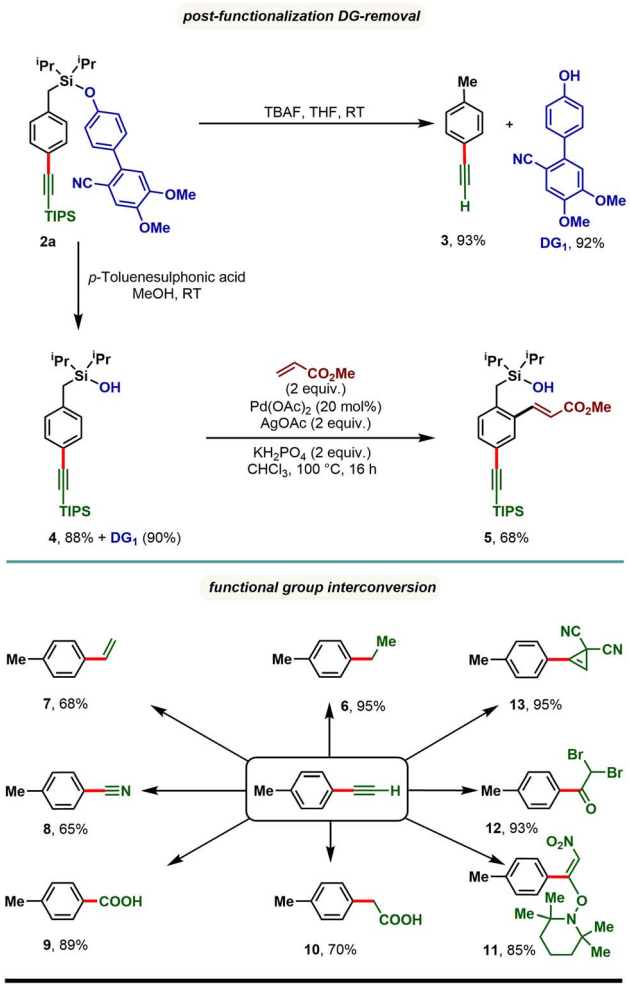

Scheme 4 Directing group (DG) removal and post-synthetic modification of *para*-alkynylated arenes.

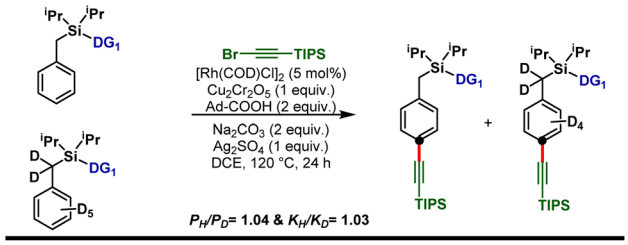

Scheme 5 Kinetic isotopic experiments with the deuterium-labeled substrate.

Isotope labeling experiments were performed involving an intermolecular competition using the substrate and its deuterated analogue d7 and a P_H/P_D value of 1.04 and k_H/k_D value of 1.03 were obtained (Scheme 5). This implies that the C–H activation step is not the overall rate-limiting step of this reaction. Furthermore, order determination studies with respect to the substrate revealed that the reaction was first order with respect to the substrate and first order with respect to the alkyne coupling partner, indicating that both the substrate and the alkyne coupling partner are involved in the rate-limiting step.

Computational studies

For computational investigation of the mechanism of present Rh-catalyzed *para*-selective C(sp^2)–H alkynylation of arenes, density functional theory (DFT) was employed. Simplified arene, **SM1**, where the isopropyl groups on the Si atom were replaced by methyl groups, and bromoethynyltriisopropyllsilane (hereafter bromoalkyne) were used for modelling. The use of ^{i}Pr groups on Si benefits from the favorable Thorpe–Ingold effect making the formation of rhodacycle easier than Me groups, but this simplification should not affect the reaction mechanism – any favorable barriers calculated with this simplified model are expected to be favorable for the ^{i}Pr analogue. The adamantane-1-carboxylate is simplified to acetate in the DFT calculations to save computational cost. The adamantyl group provides steric hinderance to the molecules and in computational modelling we avoid conformations that would give rise to clashes if adamantane-1-carboxylate were used instead of acetate. We expect the carboxylate group of the simplified acetate to provide similar metal–ligand interactions with the Rh center as the adamantane-1-carboxylate. Gibbs energy profiles were computed at the SMD (dichloroethane)-MN15 (ref. [27])/def2-QZVP//MN15/GENECP (def2-TZVPD for Br,[28] Rh[29] and Ag[29] + def2-SVP[30,31] for others) level of theory where a mixed basis set was used for geometry optimization (See ESI Section 6† for full details).[32]

The overall Gibbs free energy profile is shown in Fig. 1. First, the $Cu_2Cr_2O_5$ additive may play a role in oxidising the Rh(I) precatalyst to Rh(III) which actively participates in the catalytic cycle. Computed C–H activation barriers indicate a kinetic preference for the activation of the *para*-C–H bond (see ESI, Section 6.3†) by a factor of 16 : 1 over the *meta* position and ~1.5

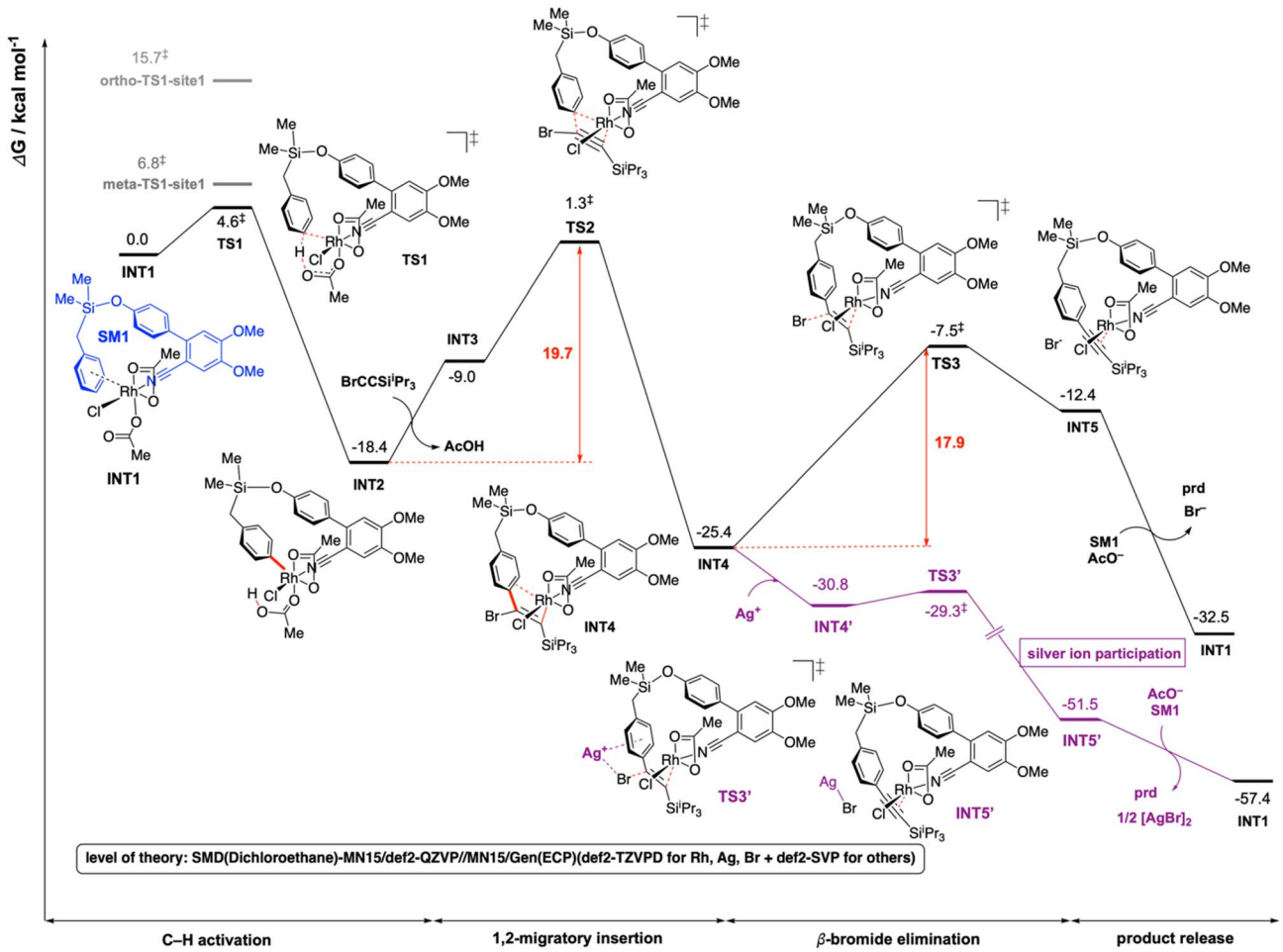

Fig. 1 Gibbs energy profile for the Rh-catalyzed C(sp^2)–H alkynylation of arenes. DFT optimized key transition structures are shown in Fig. 2.

milion : 1 over the *ortho* position. Detailed investigation of the steric and electronic influences of these TSs suggests that ring strains in the *meta*-C–H activation transition structures (*meta*-**TS1**-site1 and *meta*-**TS1**-site2, Fig. S5†) are the lowest (Table S9†) while *para*-activation has the most favorable orbital overlap between the d-orbital on Rh-metal and the π-orbital on the arene (Fig. S6†). Taken together, the activation of the *para*-C–H bond (**TS1**) is lower than the activation of the *meta*-C–H bond (by 2.2 kcal mol^{-1} for *meta*-**TS1**-site1 and by 3.9 kcal mol^{-1} for *meta*-**TS1**-site2) and the activation of the *ortho*-C–H bond (by 11.1 kcal mol^{-1} for *ortho*-**TS1**-site1 and by 13.9 kcal mol^{-1} for *ortho*-**TS1**-site2). Additionally, the C–H activation step was found not to be the turnover frequency-determining transition state (TDTS) of the reaction as the formation of the rhodacycle after C–H activation is highly exergonic and irreversible, with the subsequent barrier for 1,2-migratory insertion (19.7 kcal mol^{-1} from the C–H activated complex **INT2** to **TS2**) lower than the barrier from **INT2** back to **INT1** (23.0 kcal mol^{-1} *via* **TS1**). In the absence of silver ion participation, the *β*-bromide elimination step (**TS3**) has a barrier of 17.9 kcal mol^{-1}. In the presence of silver ions, however, the β-bromide elimination step has a much lower barrier (**TS3′**, barrier of 1.5 kcal-mol^{-1}); this is potentially favored by the exergonic formation of AgBr salt.[19a] In either case, the 1,2-migratory insertion of bromoalkyne, **TS2**, will be the overall TDTS and the C–H activated rhodacycle, **INT2**, will be the TDI. Since the bromoalkyne enters after the TDI and participates in the TDTS, this predicts a first order dependence of the reaction rate on the concentration of the bromoalkyne substrate. In addition, as the C–H activated substrate also participates in the TDTS, a first order dependence on the substrate is similarly expected from the computed energy profile. Both of these predictions are consistent with our experimental order determination measurements (first order with respect to the substrate and bromoalkyne). Finally, the alkynylation product dissociates from the catalyst–product complex **INT5′**, which releases the product and enters the next catalytic cycle by regenerating **INT1**. Combined experimental and computational mechanistic investigations suggest that the present Rh-catalyzed C(sp^2)–H alkynylation proceeds *via* non-rate-determining, irreversible regioselective C–H activation at the *para*-position, followed by turnover-frequency determining 1,2-migratory insertion of the bromoalkyne substrate. This is then followed by the β-bromide elimination step which can be greatly facilitated in the presence of silver ion participation. Our computed energy profile is in agreement with experimental kinetic isotope effects showing that C–H activation is not rate-

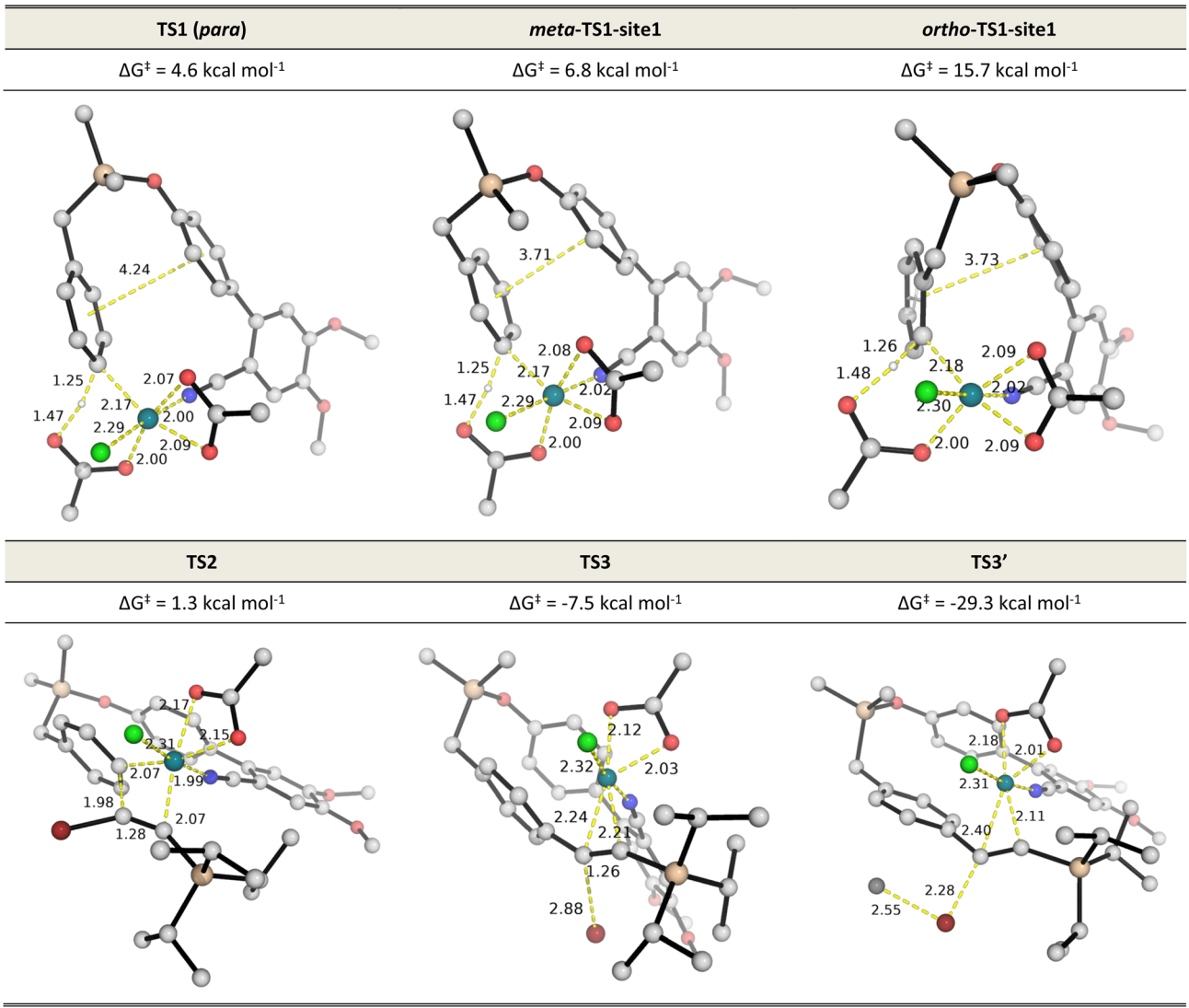

Fig. 2 DFT optimized TS structures for the C–H activation at different arene sites (**TS1**s), migratory insertion (**TS2**) and β-bromide elimination without (**TS3**) and with (**TS3′**) silver ion participation. All Gibbs energies are taken with **INT1** as zero reference. See Fig. S5† for C–H activation TSs of all possible sites.

determining and the measured rate law with first order dependence on both the substrate and the alkyne coupling partner.

Conclusions

In summary, we have developed an unprecedented route for reusable template-assisted Rh catalyzed *para*-C–H alkynylation. The protocol was well tolerated with different kinds of substituents on the arene ring. Further late-stage modification of the product and functional group inter-conversion were performed. The mechanistic studies were supported by computational studies proving that although regio-determining, the C–H activation is not the overall rate limiting step. Instead, migratory insertion of the alkyne coupling partner is overall rate-determining. We anticipate that this methodology will greatly broaden the scope of functionalization in the realm of remote *para*-C–H activation.

Data availability

Data supporting the manuscript are provided in the ESI,† including the experimental and computational methods and protocols for this study. All DFT-optimized structures have been deposited and uploaded to **https://zenodo.org/record/7585280** (DOI: **10.5281/zenodo.7585280**). Additional relevant data are available from the corresponding authors upon reasonable request.

Author contributions

U. D., G. P. and D. M. conceived the project. U. D., G. P., K. D. and K. B. completed the experimental work. X. Z. designed and

performed the computational studies and analysed the results. X. Z. and D. M. wrote the manuscript and supervised the work. All authors contributed to writing the manuscript.

Conflicts of interest

The authors declare no conflict of interest.

Acknowledgements

This activity was funded by SERB-India (TTR/2021/000108). Financial support received as fellowship from CSIR-India (to G. P.) is gratefully acknowledged. X. Z. acknowledges the support from the Agency for Science, Technology and Research (A*STAR) under its Career Development Fund (CDF Project Number C210812008) and Manufacturing, Trade and Connectivity (MTC) Young Individual Research Grants (YIRG grant number M22K3c0091) for this work. X. Z. acknowledges the partial use of supercomputers in the A*STAR Computational Resource Center (A*CRC) for computations performed in this work.

Notes and references

1 (*a*) *Acetylene Chemistry*, ed. F. Diederich, P. J. Stang and R. R. Tykwinski, Wiley-VCH, Weinheim, Germany, 2005; (*b*) *Triple Bonded Functional Groups*, ed. G. V. Boyd and S. Patai, Wiley, Hoboken, NJ, 1994, ch. 5; (*c*) H. C. Kolb, M. G. Finn and K. B. Sharpless, *Angew. Chem., Int. Ed.*, 2001, **40**, 2004–2021; (*d*) A. Fürstner and P. W. Davies, *Chem. Commun.*, 2005, 2307; (*e*) A. Fürstner, *Chem. Soc. Rev.*, 2009, **38**, 3208–3221; (*f*) M. G. Finn and V. V. Fokin, *Chem. Soc. Rev.*, 2010, **39**, 1231; (*g*) J. P. Brand and J. Waser, *Chem. Soc. Rev.*, 2012, **41**, 4165–4179; (*h*) C. Obradors and A. M. Echavarren, *Acc. Chem. Res.*, 2014, **47**, 902–912; (*i*) L. Fensterbank and M. Malacria, *Acc. Chem. Res.*, 2014, **47**, 953–965; (*j*) R. Dorel and A. M. Echavarren, *Chem. Rev.*, 2015, **115**, 9028–9072; (*k*) D. Hashmi and A. S. K. Hashmi, *Chem. Soc. Rev.*, 2016, **45**, 1331–1367; (*l*) R. Talpur, K. Cox and M. Duvic, Efficacy and safety of topical tazarotene: a review, *Expert Opin. Drug Metab. Toxicol.*, 2009, **5**, 195; (*m*) Z.-Y. Yang, J.-Q. Yuan, M.-Y. Di, D.-Y. Zheng, J.-Z. Chen, H. Ding, X.-Y. Wu, Y.-F. Huang, C. Mao and J.-L. Tang, Gemcitabine Plus Erlotinib for Advanced Pancreatic Cancer: A Systematic Review with Meta-Analysis, *PLoS One*, 2013, **8**, e57528.

2 (*a*) T. M. Swager, Semiconducting Poly(arylene ethylene)s, in *Acetylene Chemistry: Chemistry, Biology and Material Science*, ed. F. Diederich, P. J. Stang and R. R. Tykwinski, Wiley-VCH, Weinheim, 2005; (*b*) F. Diederich and Y. Rubin, *Angew. Chem., Int. Ed.*, 1992, **31**, 1101; (*c*) U. H. F. Bunz, Y. Rubin and Y. Tobe, *Chem. Soc. Rev.*, 1999, **28**, 107.

3 (*a*) L. Hintermann and A. Labonne, *Synthesis*, 2007, **8**, 1121–1150; (*b*) R. Severin and S. Doye, *Chem. Soc. Rev.*, 2007, **36**, 1407–1420; (*c*) R. Chinchilla and C. Najera, *Chem. Rev.*, 2014, **114**, 1783–1826; (*d*) J.-F. Lutz, *Angew. Chem., Int. Ed.*, 2007, **46**, 1018–1025; (*e*) M. Meldal and C. W. Tornøe, *Chem. Rev.*, 2008, **108**, 2952–3015; (*f*) A. Fürstner, *Handbook of Metathesis*, Wiley-VCH Verlag GmbH & Co. KGaA: 2015, p. 445; (*g*) J. Li and D. Lee, *Handbook of Metathesis*, Wiley-VCH Verlag GmbH & Co. KGaA, 2015, p. 381.

4 Selected examples of the Sonogashira coupling reaction: (*a*) K. Sonogashira, *J. Organomet. Chem.*, 2002, **653**, 46–49; (*b*) E. Negishi and L. Anastasia, *Chem. Rev.*, 2003, **103**, 1979–2018; (*c*) A. O. King and N. Yasuda, *Top. Organomet. Chem.*, 2004, **6**, 205–245; (*d*) H. Doucet and J.-C. Hierso, *Angew. Chem., Int. Ed.*, 2007, **46**, 834–871; (*e*) H. Plenio, *Angew. Chem., Int. Ed.*, 2008, **47**, 6954–6956; (*f*) R. Chinchilla and C. Najera, *Chem. Soc. Rev.*, 2011, **40**, 5084–5121; (*g*) R. Chinchilla and C. Nájera, *Chem. Rev.*, 2014, **114**, 1783–1826; (*h*) D. Wang and S. Gao, *Org. Chem. Front.*, 2014, **1**, 556–566.

5 For selected reviews on use of EBX see: (*a*) V. V. Zhdankin and P. J. Stang, *Tetrahedron*, 1998, **54**, 10927–10966; (*b*) V. V. Zhdankin and P. J. Stang, *Chem. Rev.*, 2008, **108**, 5299–5358.

6 For use of haloalkynes see: (*a*) A. S. Dudnik and V. Gevorgyan, *Angew. Chem., Int. Ed.*, 2010, **49**, 2096–2098; (*b*) Y. Ano, M. Tobisu and N. Chatani, *J. Am. Chem. Soc.*, 2011, **133**, 12984–12986; (*c*) Y. Ano, M. Tobisu and N. Chatani, *Synlett*, 2012, **23**, 2763–2767; (*d*) J. He, M. Wasa, K. S. L. Chan and J.-Q. Yu, *J. Am. Chem. Soc.*, 2013, **135**, 3387–3390; (*e*) K. Kobayashi, M. Arisawa and M. Yamaguchi, *J. Am. Chem. Soc.*, 2002, **124**, 8528–8529; (*f*) I. V. Seregin, V. Ryabova and V. Gevorgyan, *J. Am. Chem. Soc.*, 2007, **129**, 7742–7743.

7 Electronic controlled alkynylation: (*a*) T. de Haro and C. Nevado, *J. Am. Chem. Soc.*, 2010, **132**, 1512–1513; (*b*) Y. Wei, H. Zhao, J. Kan, W. Su and M. Hong, *J. Am. Chem. Soc.*, 2010, **132**, 2522–2523; (*c*) J. P. Brand and J. Waser, *Org. Lett.*, 2012, **14**, 744–747; (*d*) K.-Z. Deng, W.-L. Jia and M. A. Fernández-Ibáñez, *Chem. - Eur. J.*, 2021, e202104107.

8 Selected examples on DG-assisted C(sp^2)–H alkynylation with alkynyl halides: (*a*) M. Tobisu, Y. Ano and N. Chatani, *Org. Lett.*, 2009, **11**, 3250–3252; (*b*) Y. Ano, M. Tobisu and N. Chatani, *Org. Lett.*, 2012, **14**, 354–357; (*c*) M. Shang, H.-L. Wang, S.-Z. Sun, H.-X. Dai and J.-Q. Yu, *J. Am. Chem. Soc.*, 2014, **136**, 11590–11593; (*d*) F. Xie, Z. Qi, S. Yu and X. Li, *J. Am. Chem. Soc.*, 2014, **136**, 4780–4787; (*e*) H. M.-F. Viart, A. Bachmann, W. Kayitare and R. Sarpong, *J. Am. Chem. Soc.*, 2017, **139**, 1325–1329; (*f*) C. Feng and T.-P. Loh, *Angew. Chem., Int. Ed.*, 2014, **53**, 2722–2726; *Angew. Chem.*, 2014, **126**, 2760–2764; (*g*) Y.-H. Liu, Y.-J. Liu, S.-Y. Yan and B.-F. Shi, *Chem. Commun.*, 2015, **51**, 11650–11653; (*h*) N. Sauermann, M. J. Gonzalez and L. Ackermann, *Org. Lett.*, 2015, **17**, 5316–5319; (*i*) Z.-Z. Zhang, B. Liu, C.-Y. Wang and B.-F. Shi, *Org. Lett.*, 2015, **17**, 4094–4097; (*j*) Y.-J. Liu, Y.-H. Liu, X.-S. Yin, W.-J. Gu and B.-F. Shi, *Chem. - Eur. J.*, 2015, **21**, 205–209; (*k*) P. Wang, G.-C. Li, P. Jain, M. E. Farmer, J. He, P.-X. Shen and J.-Q. Yu, *J. Am. Chem. Soc.*, 2016, **138**, 14092–14099; (*l*) R. Boobalan, P. Gandeepan and C.-H. Chieng, *Org. Lett.*, 2016, **18**, 3314–3317; (*m*) V. G. Landge, G. Jaiswal and E. Balaraman, *Org. Lett.*, 2016, **18**, 812–815; (*n*) Z. Ruan, S. Lackner and L. Ackermann,

ACS Catal., 2016, **6**, 4690–4693; (*o*) Z. Ruan, N. Sauermann, E. Manoni and L. Ackermann, *Angew. Chem., Int. Ed.*, 2017, **56**, 3172–3176; (*p*) E. Tan, O. Quinonero, M. Elena de Orbe and A. M. Echavarren, *ACS Catal.*, 2018, **8**, 2166–2172and the references therein.

9 (*a*) A. Dey, S. K. Sinha, T. K. Achar and D. Maiti, *Angew. Chem., Int. Ed.*, 2019, **58**, 10820–10843; (*b*) S. Sasmal, U. Dutta, G. K. Lahiri and D. Maiti, *Chem. Lett.*, 2020, **49**, 1406–1420; (*c*) G. Meng, N. Y. S. Lam, E. L. Lucas, T. G. Saint-Denis, P. Verma, N. Chekshin and J.-Q. Yu, *J. Am. Chem. Soc.*, 2020, **142**, 10571–10591; (*d*) U. Dutta, S. Maiti, T. Bhattacharya and D. Maiti, *Science*, 2021, **372**, eabd5992; (*e*) W. Ali and G. Prakash, *Chem. Sci.*, 2021, **12**, 2735–2759; (*f*) J. Grover, G. Prakash, N. Goswami and D. Maiti, *Nat. Commun.*, 2022, **13**, 1085.

10 Y. Saito, Y. Segawa and K. Itami, *J. Am. Chem. Soc.*, 2015, **137**, 5193–5198.

11 (*a*) S. Okumura, S. Tang, T. Saito, K. Semba, S. Sakaki and Y. Nakao, *J. Am. Chem. Soc.*, 2016, **138**, 14699–14704; (*b*) S. Okumura and Y. Nakao, *Org. Lett.*, 2017, **19**, 584–587.

12 L. Yang, K. Semba and Y. Nakao, *Angew. Chem., Int. Ed.*, 2017, **56**, 4853–4857; *Angew. Chem.*, 2017, **129**, 4931–4935.

13 M. E. Hoque, R. Bisht, C. Haldar and B. Chattopadhyay, *J. Am. Chem. Soc.*, 2017, **139**, 7745–7748.

14 J. A. Leitch, C. L. McMullin, A. J. Paterson, M. F. Mahon, Y. Bhonoah and C. G. Frost, *Angew. Chem., Int. Ed.*, 2017, **56**, 15131–15135; *Angew. Chem.*, 2017, **129**, 15327–15331.

15 C. Yuan, L. Zhu, C. Chen, X. Chen, Y. Yang, Y. Lan and Y. Zhao, *Nat. Commun.*, 2018, **9**, 1189–1198.

16 C. Yuan, L. Zhu, R. Zeng, Y. Lan and Y. Zhao, *Angew. Chem., Int. Ed.*, 2018, **57**, 1277–1281; *Angew. Chem.*, 2018, **130**, 1291–1295.

17 W.-T. Fan, Y. Li, D. Wang, S.-J. Ji and Y. Zhao, *J. Am. Chem. Soc.*, 2020, **142**, 20524–20530.

18 P. Wang, G.-C. Li, P. Jain, M. E. Farmer, J. He, P.-X. Shen and J.-Q. Yu, *J. Am. Chem. Soc.*, 2016, **138**, 14092–14099.

19 (*a*) S. Porey, X. Zhang, S. Bhowmick, V. Singh, S. Guin, R. S. Paton and D. Maiti, *J. Am. Chem. Soc.*, 2020, **142**, 3762–3774; (*b*) S. Sasmal, G. Prakash, U. Dutta, R. Laskar, G. K. Lahiri and D. Maiti, *Chem. Sci.*, 2022, **13**, 5616–5621.

20 S. Bag, T. Patra, A. Modak, A. Deb, S. Maity, U. Dutta, A. Dey, R. Kancherla, A. Maji, A. Hazra, M. Bera and D. Maiti, *J. Am. Chem. Soc.*, 2015, **137**, 11888–11891.

21 (*a*) T. Patra, S. Bag, R. Kancherla, A. Mondal, A. Dey, S. Pimparkar, S. Agasti, A. Modak and D. Maiti, *Angew. Chem., Int. Ed.*, 2016, **55**, 7751–7755; (*b*) M. Li, M. Shang, H. Xu, X. Wang, H.-X. Dai and J.-Q. Yu, *Org. Lett.*, 2019, **21**, 540–544; (*c*) A. Maji, S. Guin, S. Feng, A. Dahiya, V. K. Singh, P. Liu and D. Maiti, *Angew. Chem., Int. Ed.*, 2017, **56**, 14903–14907; (*d*) A. Maji, A. Dahiya, G. Lu, T. Bhattacharya, M. Brochetta, G. Zanoni, P. Liu and D. Maiti, *Nat. Commun.*, 2018, **9**, 3582; (*e*) S. Pimparkar, T. Bhattacharya, A. Maji, A. Saha, R. Jayarajan, U. Dutta, G. Lu, D. W. Lupton and D. Maiti, *Chem. - Eur. J.*, 2020, **26**, 11558; (*f*) S. Maiti, Y. Li, S. Sasmal, S. Guin, T. Bhattacharya, G. K. Lahiri, R. S. Paton and D. Maiti, *Nat. Commun.*, 2022, **13**, 3963.

22 X. Chen, S. Fan, M. Zhang, Y. Gao, S. Lia and G. Li, *Chem. Sci.*, 2021, **12**, 4126.

23 A. Mondal, H. Chen, L. Flamig, P. Wedi and M. van Gemmeren, *J. Am. Chem. Soc.*, 2019, **141**, 18662–18667.

24 U. Dutta, S. Maiti, S. Pimparkar, S. Maiti, L. R. Gahan, E. H. Krenske, D. W. Lupton and D. Maiti, *Chem. Sci.*, 2019, **10**, 7426–7432.

25 S. Li, L. Cai, H. Ji, L. Yang and G. Li, *Nat. Commun.*, 2016, **7**, 10443–10450.

26 J. He, M. Wasa, K. S. L. Chan and J.-Q. Yu, *J. Am. Chem. Soc.*, 2013, **135**, 3387–3390.

27 H. S. Yu, X. He, S. L. Li and D. G. Truhlar, *Chem. Sci.*, 2016, **7**, 5032–5051.

28 D. Rappoport and F. Furche, *J. Chem. Phys.*, 2010, **133**, 134105–134116.

29 D. Andrae, U. Häußermann, M. Dolg, H. Stoll and H. Preuß, *Theor. Chim. Acta*, 1990, **77**, 123–141.

30 F. Weigend and R. Ahlrichs, *Phys. Chem. Chem. Phys.*, 2005, **7**, 3297–3305.

31 F. Weigend, *Phys. Chem. Chem. Phys.*, 2006, **8**, 1057–1065.

32 M. J. Frisch, G. W. Trucks, H. B. Schlegel, G. E. Scuseria, M. A. Robb, J. R. Cheeseman, G. Scalmani, V. Barone, G. A. Petersson, H. Nakatsuji, *et al.Gaussian 16, Revision B.01*. 2016.